

## Special Issue – Imaging Cell Biology

# Soft X-ray tomography and cryogenic light microscopy: the cool combination in cellular imaging

Gerry McDermott<sup>1</sup>, Mark A. Le Gros<sup>2</sup>, Christian G. Knoechel<sup>1</sup>, Maho Uchida<sup>1</sup> and Carolyn A. Larabell<sup>1,2</sup>

<sup>1</sup>Department of Anatomy, University of California San Francisco, CA 94143, USA

<sup>2</sup>Physical Biosciences Division, Lawrence Berkeley National Laboratory, Berkeley, CA 94720, USA

**Soft X-ray tomography (SXT) is ideally suited to imaging sub-cellular architecture and organization, particularly in eukaryotic cells. SXT is similar in concept to the well-established medical diagnostic technique computed axial tomography (CAT), except SXT is capable of imaging with a spatial resolution of 50 nm, or better. In SXT, cells are imaged using photons from a region of the spectrum known as the 'water window'. This results in quantitative, high-contrast images of intact, fully hydrated cells without the need to use contrast-enhancing agents. The cells that are visualized are in close-to-native, fully functional state. The utility of SXT has recently been enhanced by the development of high numerical aperture cryogenic light microscopy for correlated imaging. This multi-modal approach allows labelled molecules to be localized in the context of a high-resolution 3-D tomographic reconstruction of the cell.**

## Introduction

Our understanding of cell structure and behaviour has been particularly dependent on imaging. As a consequence, the emergence of new imaging modalities potentially leads to new insights and discoveries in cell biology. In this review, we examine soft X-ray tomography (SXT), an emerging technique for quantitatively imaging whole, hydrated cells in 3-D. SXT imaging is both unique and complementary to existing imaging techniques, such as light and electron microscopy. The soft X-ray (see Glossary) illuminating photons used in SXT penetrate biological materials much more easily than electrons, which allows specimens up to 10  $\mu\text{m}$  thick to be imaged. Unlike electron microscopy, this means there is no need to section eukaryotic cells with an ultramicrotome before imaging by SXT. Since contrast in SXT is produced directly by the differential absorption of X-rays, there is no need to dehydrate or stain specimens. Consequently, SXT produces high-resolution views of specimens in a near-native state. Recently, SXT was made even more powerful by the development of high numerical aperture cryogenic light microscopy for correlated imaging. This combination of light and X-ray modalities allows tagged molecules to be localized in the context of a high-resolution,

3-D image of a cell. This meets a long-standing need in cell research and, as such, has enormous transformational potential in academic, industrial and clinical research.

We begin by reviewing the development of soft X-ray microscopy for biological imaging, and then describe the extension of this technique to 3-D tomographic imaging.

## Soft X-ray microscopy

X-ray microscopes have been used for materials science research since the 1940 s [1]. However, only since the 1990 s has the technique become capable of satisfactorily

## Glossary

**Alignment:** The adjustment of projection images in a rotation (tilt) series to account for physical shifts in the specimen holder during the collection of a rotation series; due to imperfect instrumentation.

**ALS:** The Advanced Light Source, Berkeley, California. A third generation synchrotron, and the world's brightest source of soft X-rays (<http://als.lbl.gov>)

**ART:** Algebraic reconstruction technique. An iterative algorithm used to reconstruct 3-D volumes from 2-D projection images.

**BESSY:** The Berliner Elektronenspeicherring-Gesellschaft für Synchrotronstrahlung. A synchrotron X-ray light source in Berlin, Germany (<http://bessy.de>) Note, BESSY has been renamed as Helmholtz-Zentrum Berlin für Materialien und Energie GmbH

**Cryo-fixation:** Cooling the specimen by methods that prevent water from turning into crystalline ice.

**Filtered back-projection:** A technique for tomographic reconstruction where the projection rays are 'back-projected' through Fourier space to form the 3-D volume.

**LAC:** Linear absorption coefficient. The fraction of a beam of radiation absorbed per unit thickness of absorber, as defined by the Beer–Lambert law.

**NCXT:** The National Center for X-ray Tomography (<http://ncxt.lbl.gov>).

**Orthoslice:** An orthoslice is an extraction of absorption values along a plane perpendicular to one of the coordinate axes (in other words, the generation of a 2-D representation from a 3-D volume). The complete reconstructed volume of the specimen consists of a number of such planes.

**Projection image:** An individual image from a rotation (tilt) series.

**Rotation series:** A number of projection images that have been collected around a rotation axis.

**SXT:** Soft X-ray tomography.

**Soft X-rays:** Photons with wavelengths of one to several nanometres, and energies up to 1 keV.

**Tilt series:** Synonymous with rotation series, more commonly used in electron tomography.

**Tomographic reconstruction:** Computationally combining aligned projection images from a rotation (tilt) series to form a 3-D volumetric reconstruction of the specimen.

**Water window:** The region of the electromagnetic spectrum that lies between the K shell absorption edges of carbon (284 eV,  $\lambda=4.4$  nm) and oxygen (543 eV,  $\lambda=2.3$  nm).

**Zone plate:** Diffractive lenses used in soft X-ray microscopes (see Box 1).

Corresponding author: Larabell, C.A. ([Carolyn.Larabell@UCSF.edu](mailto:Carolyn.Larabell@UCSF.edu)).

imaging biological specimens [2–5]. At this point, soft X-ray microscopes operating in the ‘water window’ region of the spectrum began to be equipped with high-efficiency CCD cameras. The advances resulted in the production of projection images with stunning clarity and contrast from a range of cells and tissue specimens [6–8].

Soft x-ray microscopes have three clear advantages over light and electron microscopes. Firstly, the short wavelength allows cells to be imaged at significantly higher spatial resolution than is possible with light. Secondly, fully hydrated specimens up to 10  $\mu\text{m}$  thick can be imaged without the need for sectioning [9–13], and finally, image contrast is obtained directly from the absorption of X-rays by the specimen. The water window is the region of the spectrum that lies between the K shell absorption edges of carbon (284 eV,  $\lambda=4.4$  nm) and oxygen (543 eV,  $\lambda=2.3$  nm). Photons within this energy range are absorbed an order of magnitude more strongly by carbon- and nitrogen-containing organic material than by water [9]. This absorption adheres to Beer-Lambert’s Law and is therefore linear with thickness and concentration [5]. Consequently, images produced by soft X-ray microscopes are quantitative, with each biochemical component having a signature X-ray linear absorption coefficient (LAC) [9,12]. As a result,

cell structures are visualized directly, with image contrast being derived from differences in biochemical composition and density. For example, dense lipid-rich structures exhibit significantly greater X-ray absorption than organelles such as vacuoles that have significant water content.

The optical arrangement of a soft X-ray microscope is relatively simple, and similar in concept to that of a simple bright-field microscope. A condenser lens illuminates the specimen and an objective focuses the transmitted light onto a detector. This optical configuration is shown in simplified form in Figure I in Box 1. The physical characteristics of soft X-rays preclude the use of Conventional glass lenses. Instead, soft X-ray microscopes rely on Fresnel zone plates or X-ray focusing capillaries (see Figure II in Box 1) [5,14,15].

Before being imaged in a soft X-ray microscope, cells must be mounted in a suitable holder. This is typically a thin-walled glass capillary tube or a flat silicon nitride membrane. Capillary holders have the advantage of permitting the specimen to be rotated through 360°. Depending on the magnification, the field of view in a soft X-ray microscope is up to 15  $\mu\text{m}$ , allowing multiple cells to be imaged per data set. In the case of bacteria this can be tens or even hundreds of cells per experiment. With larger,

### Box 1. The optical arrangement of a soft X-ray microscope

#### Optical layout of a soft X-ray microscope

The optical configuration of XM-2, a soft X-ray microscope used for biological and biomedical tomography at the National Center for X-ray Tomography [9] is shown in Figure I. Polychromatic X-rays from a synchrotron ‘bend magnet’ are steered to the condenser by a mirror. In this configuration, a condenser lens focuses the X-rays onto the specimen and functions as a monochromator. The objective lens generates a magnified image of the specimen on the detector. In this instrument, the condenser and objective optics are Fresnel zone plates. In other instruments, ‘undulators’ are used in place of ‘bend magnets’ as the X-ray source [33], and ‘rotating condensers’ [34] or ‘capillaries’ [26] are used in place of zone plates as the condenser.

#### Lenses for soft x-ray microscopy

Soft X-ray microscopes use Fresnel zone plates either as both condenser and objective lenses, or only as the objective. Unlike a conventional lens, a zone plate relies on diffraction rather than refraction to focus the light [5]. Zone plates consist of radially symmetric rings, known as Fresnel zones, which alternate between opaque and transparent (see Figure II). Currently, the highest resolution zone plates available have an outer width of 15 nm [32,35]. In a soft X-ray microscope, such as XM-2, the spatial resolution obtained is determined by the outer width of the objective zone plate [5].

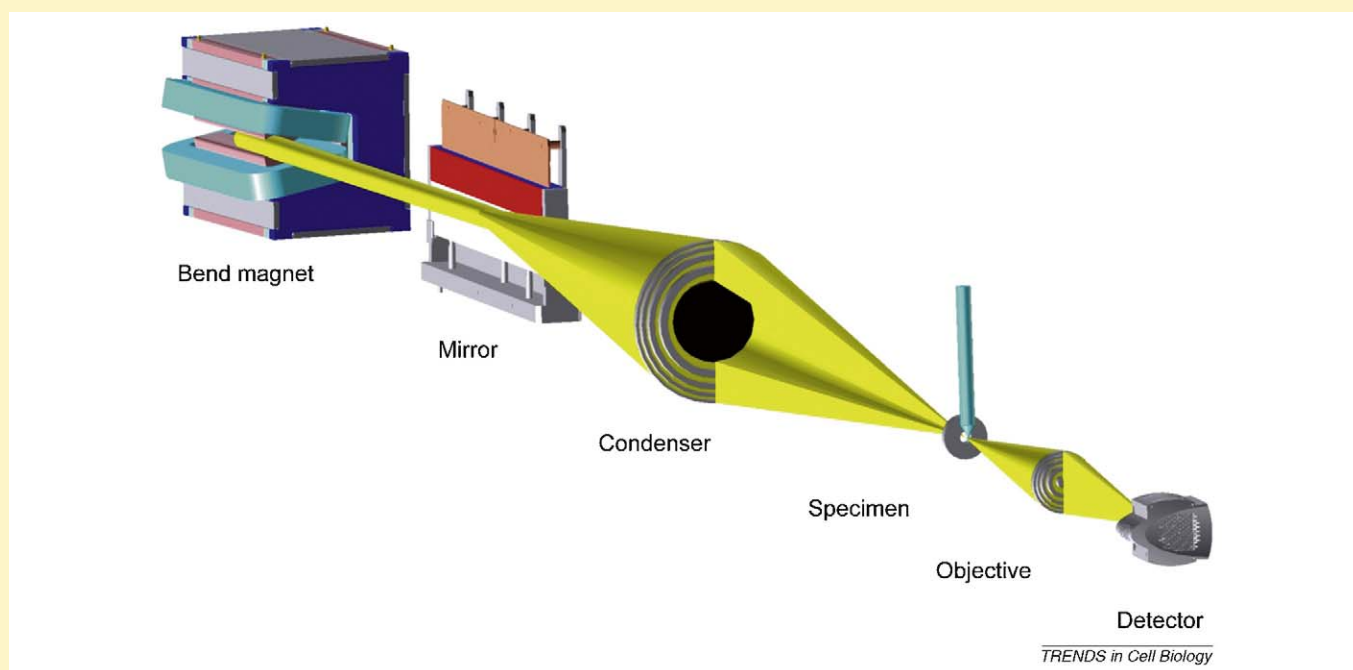
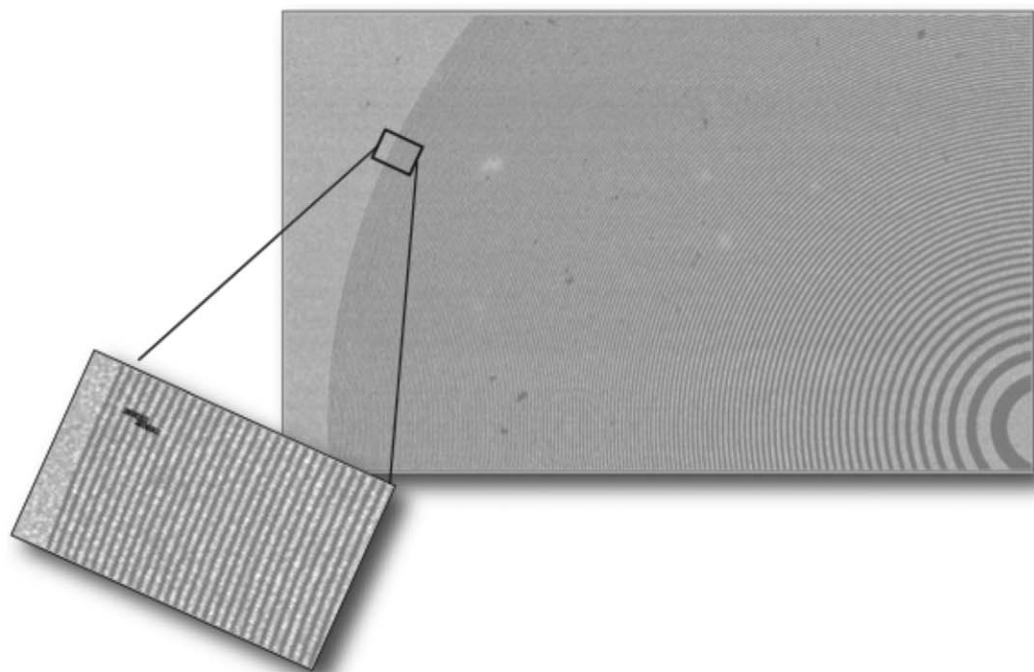


**Figure I.** Schematic representation of the main components in XM-2, a new soft X-ray microscope designed for cellular imaging.



TRENDS in Cell Biology

**Figure II.** Scanning electron micrograph of a Fresnel zone plate [5]. The inset shows the outermost zones in close-up.

higher-order cells, such as yeast, each tomographic data set typically contains three to seven cells. This compares very favourably with electron tomography, where cells must first be cut into sections that are a maximum of 200–500 nm thick, either using a microtome, or by ion milling [16]. This is an onerous task and was identified in a recent review as being the ‘Achilles heel of electron tomography’ and the underlying reason why so few cells

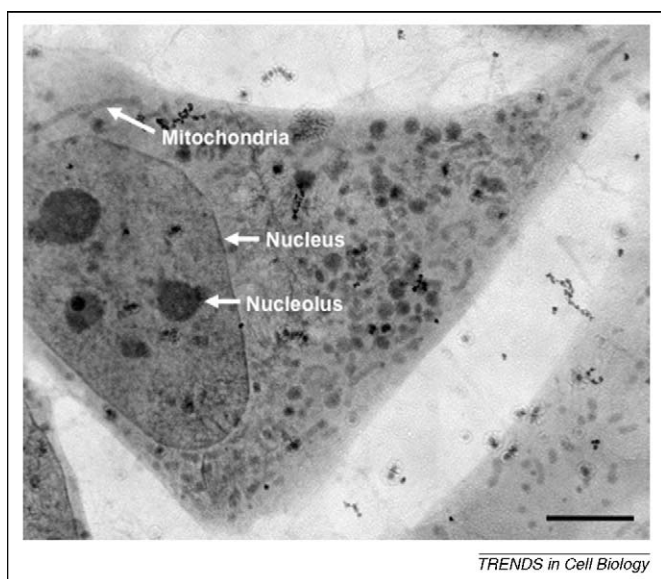
have been imaged in 3-D using this technique [13]. Consequently, SXT represents a significant leap forward in terms of the ability to visualize cells.

### Soft X-ray Tomography

As with light and electron microscopes, a soft X-ray microscope can only produce 2-D representations of a 3-D specimen. Such images can, of course, be very informative (see Figure 1) and in the past they have provided insights into the general structure and organization of various types of cells [5,6,8,17]. However, for most biological specimens 2-D imaging results in structural features being confusingly superimposed, rendering high-resolution projection images of complex eukaryotic cells virtually meaningless [9,11,18,19]. However, if a sufficient number of 2-D images are recorded at incremental angles around a rotation or ‘tilt’ axis a 3-D tomographic reconstruction of the specimen can be calculated [13,18,20,21]. The principles of tomography are described briefly in Box 2.

### Evolution of the cryogenic rotation stage for tomography

All biological materials are eventually damaged when they are exposed to intense sources of radiation, irrespective of whether this is ultraviolet illumination in a fluorescence microscope, electrons in an electron microscope, or photons in an X-ray microscope. Tomographic imaging requires a number of projection images to be collected from the same specimen. Therefore, steps must be taken to mitigate the effects of radiation damage. The most efficient way to do this is to mount the specimen in a cryogenic stage and image it after vitrification. The first cryogenic specimen stages designed for soft X-ray microscopy did not permit



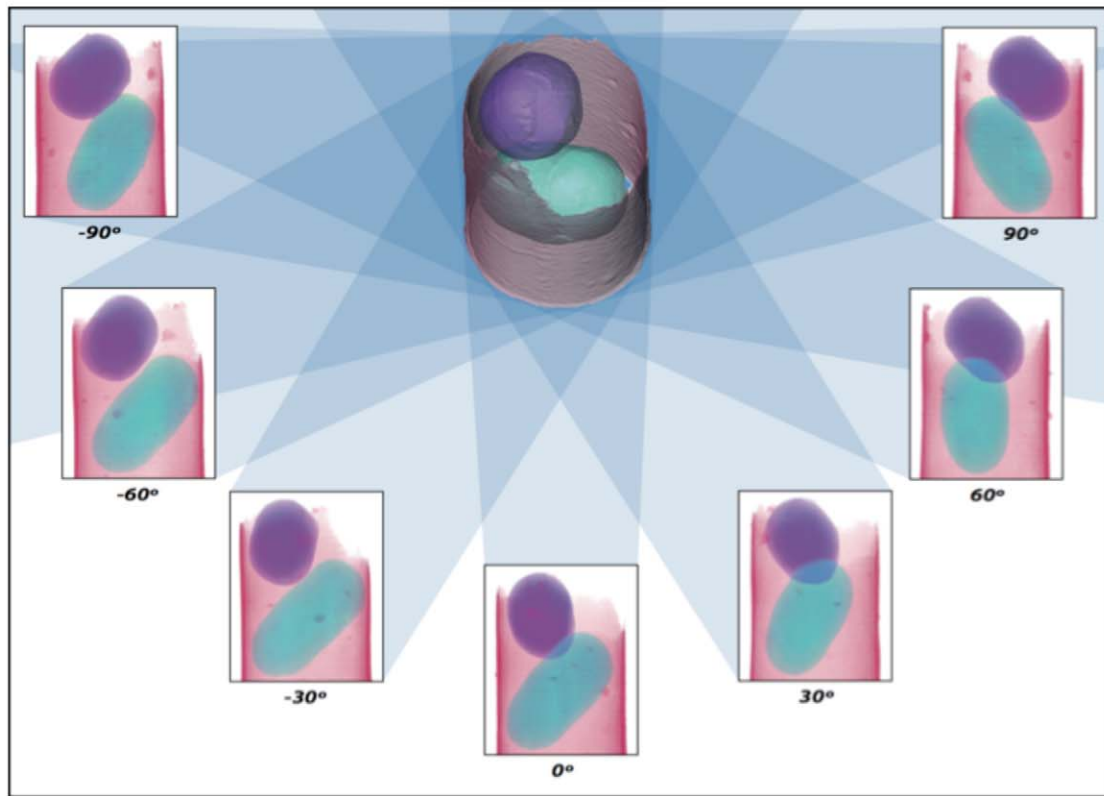
TRENDS in Cell Biology

**Figure 1.** Soft X-ray projection image of cryo-fixed NIH 3T3 cells. In this image the contrast is generated by absorption of ‘water window’ X-ray photons by the carbon and nitrogen in the nuclear and cytoplasmic organelles, and not by the use of metal stains. Consequently, the information obtained by this method is quantitative and represents the specimen in a close-to-native state. The scale bar represents 5  $\mu$ m. (from Ref. [6]).

**Box 2. The basic principles behind tomographic reconstruction**

In Figure 1 in Box 2, projection images of two yeast cells mounted in a glass capillary tube are taken at angular increments around a rotation axis. For clarity, projection images are shown at 30° intervals; in practice, images are collected at much smaller angular increments, typically every 1 or 2° over a total range of 180°. The projection images are then used to calculate a 3-D reconstruction of the

specimen either by filtered back projection [36] or by algebraic reconstruction techniques (ART) [37]. In this figure, the two yeast cells are coloured teal and purple, and the glass capillary is in red. Tomographic data are greyscale in general. The central reconstruction shows the same two cells, complete with the surrounding capillary specimen holders.



TRENDS in Cell Biology

**Figure 1.** A 3-D reconstruction of two yeast cells in a glass capillary (top centre) calculated from 2-D projections collected sequentially around a rotation axis (shown at 30° increments).

the specimen to be rotated around an axis. However, it was possible to use these instruments to collect enough images from a specimen to show that cryo-cooling does indeed reduce radiation damage to the point that tomography is feasible [6,22,23].

More recently, two cryogenic stages capable of rotation were developed independently (one by the Schmahl group at the BESSY 1 synchrotron in Berlin, the other by Larabell and Le Gros at the National Center for X-ray Tomography (NCXT) at the Advanced Light Source (ALS), Berkeley). The first tomographic images of cells produced by these instruments energized the community by providing glimpses of what could be achieved with this technique [10,12,24,25]. The cryo-rotation stage developed at the NCXT has the advantage of holding the specimen at atmospheric pressure, rather than retaining it in a vacuum (as is the case with the adapted electron microscope (EM) cryo-stage described in Ref. [26]). By bathing the specimen in cryogenic helium, heat is transferred efficiently, thus keeping the specimen vitrified at a stable temperature throughout data collection. In addition, this configuration of cryo-rotation stage allows the ready incorporation of

other imaging modalities. In the past year, the NCXT cryo-rotation stage has proven to be a reliable workhorse that has produced the data for several thousand tomographic reconstructions of cells. A representative of these reconstructions is shown in Figure 2, together with light microscopy images of similar cells for comparison.

**Soft X-ray tomography: applications**

The beauty of SXT is that it can be applied to virtually any imaging problem in cell biology, from imaging simple bacteria, to visualizing the internal structure of high-order eukaryotic cells and even tissue specimens. The first reported soft X-ray tomographic reconstruction was of the alga *Chlamydomonas reinhardtii* [12,25]. This was a landmark publication for the development of the field, and showed that cryogenically cooling mitigated radiation damage sufficiently to allow biological cells to be tomographically imaged with high fidelity. Even to this day, this work by Weiss and colleagues stands as an exceptional example of what can be achieved with SXT.

In later work, Larabell and colleagues carried out a number of studies on both fission and budding yeasts



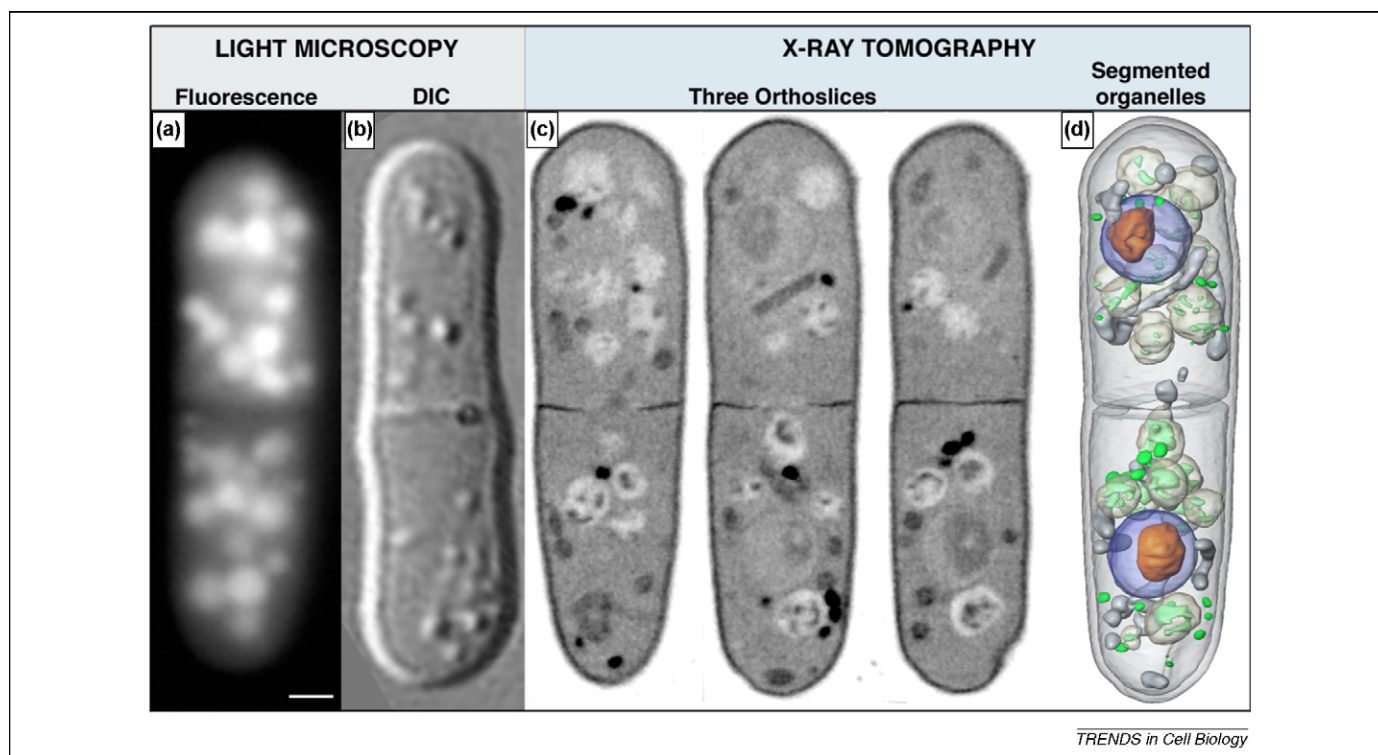


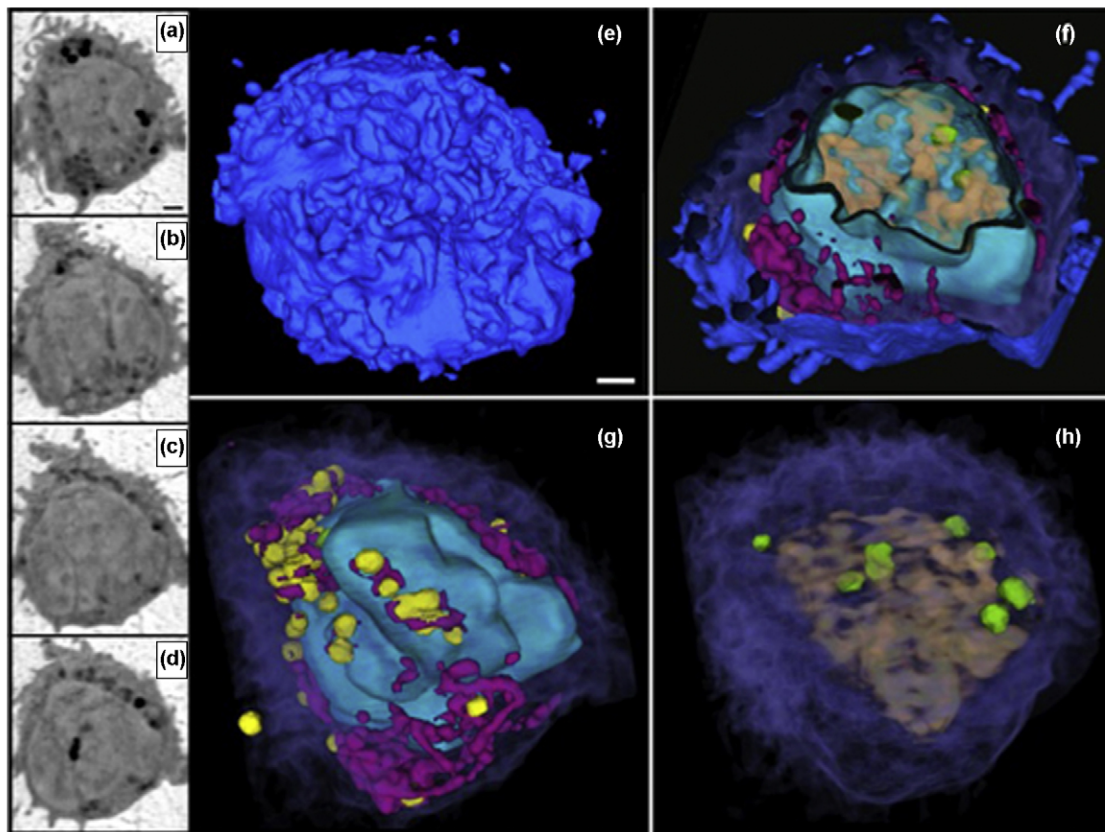
**Figure 2.** Comparative images of the fission yeast *Schizosaccharomyces pombe* using light and soft X-rays. (a) Conventional fluorescence microscopy (vacuoles labelled with CellTracker Green CMFDA (5-chloromethylfluorescein diacetate) from Invitrogen). (b) Differential interference contrast (DIC) light microscopy. (c) Orthoslices (see the Glossary) through a soft X-ray tomographic reconstruction. (d) The reconstruction in (c) after segmentation. Organelles are identified by their characteristic shape and measured X-ray linear absorption coefficients (LAC). Key: nucleus, blue; nucleolus, orange; mitochondria, grey; vacuoles, white; lipid-rich vesicles, green. (X-ray tomographic reconstructions are an update of the work outlined in Refs [27,28]). The scale bar represents 1  $\mu\text{m}$ .

[24,27,28]. Data were collected for these publications using a prototype cryo-rotation stage mounted on XM-1, a general-purpose soft X-ray microscope at the ALS. Since XM-1 was used primarily for magnetism and materials research, it was not optimally configured for biological imaging. The images produced in these studies were, however, highly informative and helped guide the specimen-handling protocols and data collection strategies used in later work.

After the commissioning of an XM-2 in 2008, the earlier work of Larabell and colleagues was quickly surpassed. In addition to having an optical system optimized for biological imaging, incorporated into the new microscope is a second-generation cryo-rotation stage that contains a large number of improvements over the prototype. For example, it has much greater mechanical and thermal stability. The combination of new microscope and cryostage has led to improved image quality and fidelity. As a representative example of the capability of this new facility, some recent imaging of T-cells is shown in Figure 3 and the morphological differences in the yeast *Candida albicans* are shown in Figure 4. Of particular note is the ability to tomographically image cells that exceed the field of view, such as the *Candida* hyphal cell shown in Figure 4. This cell measured 47  $\mu\text{m}$  lengthwise (and 2–3  $\mu\text{m}$  in width along the hyphal tube). The cell was mounted in a thin-walled glass capillary and it was a straightforward procedure to collect five successive fields of view, and thus image the entire cell. In this study, each field of view was reconstructed individually before being ‘stitched’ together *in silico* to form a composite image of the entire cell. Imaging a cell this size using EM tomography is an impossible

challenge, since it would require imaging approximately 200 sections of the same hyphal cell. Using soft X-ray microscopy, the projection images necessary to complete this enormous reconstruction were collected in less than 20 minutes.

In a soft X-ray microscope, such as XM-2, the observed spatial resolution is determined by the zone plate optical elements (see Figure II in Box 1). In microscopes that utilize alternate condensers, the factors that determine spatial resolution are more complicated and beyond the scope of this review (however, it should be noted that microscopes with capillary condensers, such as the one in BESSY, currently have the potential to image with a spatial resolution of better than 20 nm). Most SXT studies have used zone plates that produce images with a spatial resolution of 50–60 nm. As with all imaging modalities, there is much debate in the scientific community regarding spatial resolution; indeed, one might assume that the resolution limit is the ultimate criterion of quality in any imaging technique. In a recent review, Leis and colleagues directly questioned this assumption [13]. In their opinion, measurement of the absolute resolution limit is a rather academic exercise and of limited importance compared to determining how much useful information can be obtained from an imaging technique, or how well this correlates with ‘reality’. In other words, the most important considerations are “can the imaging technique under consideration adequately answer the questions being posed?” and “are the images produced by it a true representation of the live, fully functional specimen?” Leis and colleagues also proposed that ‘direct’ imaging techniques



TRENDS in Cell Biology

**Figure 3.** X-ray tomography of a lymphocyte (T-cell). (a–d) Orthoslices from the tomographic reconstruction of a cryo-fixed T-cell imaged in a capillary. (e–h) Segmented volumes. (e) Cell surface with numerous filopodial extensions. (f–h) Cut-away views showing the typical highly folded large nucleus (cyan) surrounded by a small rim of cytoplasm (purple). Multiple highly absorbing vesicles (yellow) surround the nucleus (cyan), along with less absorbing structures, including mitochondria (magenta) in the cytoplasm. Chromosomes (salmon) and nuclear bodies (green) are seen in the nucleus. The diameter of the cell is 8  $\mu\text{m}$ . The scale bar represents 1  $\mu\text{m}$ .



TRENDS in Cell Biology

**Figure 4.** Tomographic imaging of the three phenotypes displayed by the yeast *Candida albicans*. (a) Yeast-like cells; (b) pseudo-hypha; and (c) hypha. Images after segmentation of the major organelles are shown. The measured linear absorption coefficients for the segmented organelles are given in Table 1. The hyphal cell, shown in (c) has a total length of 47  $\mu\text{m}$ . Five tomographic data sets were collected sequentially along the length of the cell. These were 'stitched' together after reconstruction using the software package Amira from Visage Imaging Inc. Key: nucleus, blue; nucleolus, purple; mitochondria, orange; vacuoles, yellow; lipid drops, dark green. The scale bar represents 1  $\mu\text{m}$ . After figures in M. Uchida *et al.*, PNAS, in press.

are significantly more informative and produce more accurate representation of the specimen than 'indirect' imaging of specimens. In this context, direct imaging methods are those that rely on intrinsic properties of the specimen, such as the absorption of X-rays according to biochemical composition or density to form the image. Whereas indirect

methods are those where specimens are stained before imaging, in which case it is actually the stain that is imaged rather than the specimen *per se*. How accurately this represents the specimen is a function of factors such as how well the individual components in a cell bind the stain, which is obviously an unknown. On the other hand, SXT is

### Box 3. Segmentation

Segmentation is the process of computationally isolating, visualizing and quantifying specific cellular components, such as the cytoskeleton or organelles, in a tomographic reconstruction. Each voxel in a soft X-ray tomographic reconstruction is a direct measurement of the X-ray linear absorption coefficient (LAC) at the corresponding location in the cell. Since biological materials absorb soft X-rays according to Beer's Law, the LAC values for similarly sized voxels depend solely on the concentration and composition of biomolecules present, with water having an order of magnitude lower LAC than molecules such as lipids and proteins. LAC values for homogeneous solutions of isolated biomolecules can be readily measured or calculated. For example, pure water in the form of ice was calculated to have an LAC of  $0.109 \mu\text{m}^{-1}$ , whereas a model protein with the chemical composition  $\text{C}_{94}\text{H}_{139}\text{N}_{24}\text{O}_{31}\text{S}$  was calculated to have a theoretical LAC of  $1.35 \mu\text{m}^{-1}$  [12]. In practice, most of the voxels in a 50 nm resolution soft X-ray reconstruction of a cell will contain a heterogeneous mixture of biomolecules. Using a measurement at a single wavelength makes it impossible to distinguish the chemical composition of a heterogeneous mixture unambiguously. However, most organelles and cellular structures are sufficiently similar in their biochemical composition to allow them to be identified and differentiated from the surrounding cell contents. For example, the relatively high water content in vacuoles makes them readily distinguishable from organelles that are more dense in biomolecules, such as nuclei and mitochondria.

Even relatively small variations in organelle LAC can be distinguished; for example, the boundaries between nuclei and nucleoli are very clear.

Segmentation can be done manually or semi-automatically. Manual segmentation is done interactively by outlining regions of interest based on a threshold of the absorption value or by visual inspection. Alternatively, a cell can be segmented completely into sub-volumes by more automatic methods. The software tools used for this task use absorption values and/or the magnitude of gradients between regions in the reconstruction. A variety of standard image manipulation approaches, such as smoothing and edge detection techniques, are routinely used. Starting with a user-defined threshold of the absorption values, or some interactively defined seed points, and using region-growing algorithms, regions of interest can be defined and delineated. If necessary, watershed or level set methods can be used to further define the borders of specific sub-cellular components. For further information see, for example, the itk Insight Toolkit at <http://www.itk.org>.

Once the cell has been segmented, *a priori* knowledge such as size, position inside a cell, boundary conditions, and so on can be used to aid identification of the segmented volumes. With recently developed instrumentation it is now possible to achieve correlated high-resolution light and X-ray tomographic imaging on the same specimen. This will permit unambiguous assignment of additional organelle identities to segmented volumes [29].

a direct imaging method with minimal specimen preparation requirements, and therefore maximal retention of specimen integrity.

Another positive attribute of SXT is that it produces isotropic data. This is particularly true when the specimen is mounted in a capillary that can be rotated freely without angular limitation. Cells that are too large to fit into capillaries are mounted on flat silicon nitride specimen holders. Due to instrumental limitations, these holders do not have completely unlimited angular rotation; however, this limitation is minimal and does not have a significant impact on the fidelity of the reconstruction. In contrast, tilting the specimen in EM tomography causes it to become 'thicker' than the depth through which the electrons can penetrate. This places rather restrictive limitation on the maximum tilt, resulting in a significant wedge of missing data. This reduces the signal-to-noise in EM tomographic reconstructions, and makes techniques such as automatic segmentation significantly more difficult to apply.

The excellent signal-to-noise in an SXT tomogram makes it relatively straightforward to segment a reconstructed cell into organelles and other sub-cellular structures based on their LACs (Box 3). Table 1 gives the measured average LACs for organelles in the segmented *C. albicans* cells shown in Figure 4. It should be clear from these data that, for example, mitochondria are readily distinguishable from lipids or vacuoles.

Whilst informative, the LAC values alone cannot give information on the location of specific molecules, which

requires the molecules to be tagged and visualized directly with SXT, or by the use of a correlated microscopy method.

### Localizing molecules using correlated cryogenic light microscopy

Determining the location of specific molecules and complexes in a cell is one of the keystones of modern cell biology. However, the combination of localization data with structural imaging is even more informative than either technique alone. SXT has the potential to play a major role in this regard. Molecules can be localized directly in a tomographic reconstruction of a cell by immuno-labelling them with electron-dense tags [6]. This type of labelling has been very well developed for use in electron and light microscopy. However, there are distinct disadvantages to immuno-labelling. Typically, the specimen is chemically fixed and then treated with membrane-permeabilizing agents, such as detergents or organic solvents, to allow the relatively large antibodies to enter the interior of the cell. Obviously, disrupting the integrity of membranes to allow large molecules to enter the cell results in a significant leakage of proteins and other molecules out of the cell, potentially causing serious damage to the specimen. Furthermore, once inside the cell, the antibodies may have limited, or no, access to the target epitope-containing molecules.

A less damaging method for localizing molecules is to use genetically encoded labels, such as a fluorescent protein (FP), to localize molecules of interest using fluorescence microscopy, and correlate these data with SXT. In a recent paper, Le Gros and colleagues describe the development of cryogenic high numerical aperture light microscopy, and its integration with SXT [29]. This microscope has been integrated into the NCXT cryo-rotation stage to allow correlated light and X-ray imaging of the same specimen.

**Table 1. Measured, average (AVG) LACs for organelles in the segmented *Candida albicans* cells**

	AVG LACs ( $\mu\text{m}^{-1}$ )
Lipid droplets	$0.75 \pm 0.09$
Mitochondria	$0.45 \pm 0.03$
Nuclei	$0.28 \pm 0.03$
Nucleoli	$0.37 \pm 0.04$
Vacuoles	$0.20 \pm 0.03$



**Box 4. Localizing molecules in a soft X-ray reconstruction of a cell**

Molecules can be tagged and localized in a soft X-ray reconstruction by two distinct methods; either directly in the tomogram using electron-dense, metal tags or by tagging the molecule with a fluorescent moiety and using correlated light microscopy.

**Direct:** The direct method is the least favoured because this generally requires the cell to be fixed and the membranes permeabilized to allow a tag, which is normally conjugated to an antibody, to enter the cell. An advantage to this method is that it examines the position of native proteins and uses modified protocols and commercially available reagents developed for other imaging modalities (such as those described in Ref. [38]). For example, these electron-dense tags have been generated using 1.4 nm gold-conjugated secondary antibodies. Followed by enhancement with silver to produce metal tags that were approximately 50 nm in diameter [6]. More recently, nanoparticles, such as TiO<sub>2</sub>, have been used as tags [39]. These tags have the advantage of having an X-ray absorption edge in the region of the water window. This allows two tomographic data sets to be collected; one at an energy corresponding to an X-ray

absorption maximum of titanium, the other at lower energy. Calculation of a difference tomogram allows the position of the labelled molecules in the cell to be determined accurately.

**Correlated:** High numerical aperture correlated light microscopy is a very recent development [29]. In this technique, the specimen is cryo-fixed and then imaged using both fluorescence and soft X-ray methods. The latter visualized the cellular architecture into which the fluorescently tagged molecules can be localized. There are a number of very significant advantages to this method. First, tagging with fluorescence molecules is a mainstay of biology that can be readily applied to most cell types, with the ability to tag multiple molecules in the same experiment [40,41]. Second, the specimen does not have to be processed in any way, which eliminates the possibility of structural damage. Third, imaging the same specimen using two different modalities eliminates ambiguities during interpretation. Finally, the fluorescence signal can be monitored before cryo-fixation using live cell imaging until the appropriate state has been reached, or to permit selection of a specimen with specific characteristics.

**Future directions**

Soft X-ray tomography is now living up to long-held expectations as a high-resolution, 3-D imaging technique capable of visualizing intact eukaryotic cells in a close-to-native state [13]. Furthermore, the latest cryo-rotation stages allow a large number of cells to be imaged quantifiably in a very short space of time, making SXT ideally suited to generating statistically significant quantities of phenotypic data.

Several new SXT instruments are either under construction or being considered for construction at synchrotrons around the world<sup>a</sup>. Rapid progress is now being made on the development of 'table-top' X-ray sources with characteristics that make them suitable for use as sources for soft X-ray microscopy [30,31].

As discussed above, the absolute spatial resolution achieved using an imaging technique such as SXT is not the major consideration. That said, there are clearly some particular situations where SXT imaging can benefit from increased spatial resolution. Fortunately, advances in nanofabrication technologies can be applied to manufacturing zone plates with incrementally higher spatial resolution. The current generation zone plates have a maximum spatial resolution of 15 nm [32]. These enhanced resolution optics are easily incorporated into existing soft X-ray microscopes. However, concomitant with an increase in resolution, there is a decrease in the depth of field. With zone plates with a resolution better than 25 nm, the depth of field is smaller than the thickness of most eukaryotic cells. Overcoming this limitation requires the development of computational methods and the use of modified data collection strategies. The most obvious solution is to use established methods such as deconvolution to overcome the depth of field limitations. This combination of deconvolution and tomography (DETOMO) is computationally straightforward and relies on adaptation of existing code, rather than the development of completely new algorithms (Le Gros *et al.*, unpublished observation).

Similar to macromolecular crystallography, SXT is highly amenable to automation and remote operation. Currently, SXT facilities, such as the NCXT, are in the process of installing robots capable of mounting specimens, and implementing software to automatically collect, process and archive data. There are a number of advantages to automation, besides making life easier for the experimenter. Most biological experiments are time and/or cell cycle-dependent. Consequently, it is essential that specimens can be collected, cryo-fixed and stored. Much work is being directed towards automating segmentation, one of the current bottlenecks in both EM tomography and SXT. In general, software packages developed for EM tomography can be used for SXT data without modification; however, since SXT produces isotropic data with excellent signal-to-noise ratios, there is a need for software optimized for SXT to take full advantage of these unique characteristics.

Perhaps the most exciting recent development in SXT imaging is the correlated use of X-ray and cryo-light microscopy [29]. Using this combination of modalities, it is possible to determine the location of labelled proteins using fluorescence, and then place this information directly into a high-resolution tomographic reconstruction of the cell (Box 4). This represents an enormous leap forward in our ability to image cells, and cellular processes.

**Acknowledgements**

We acknowledge the assistance of Drs Dula Parkinson and Markko J. Myllys in the preparation of the Figures. This work was funded by the US Department of Energy, Office of Biological and Environmental Research (DE-AC02-05CH11231), the National Center for Research Resources of the National Institutes of Health (RR019664) and the National Institutes of General Medical Sciences of the National Institutes of Health (GM63948).

M.A.L. and C.A.L. are the inventors on patents for the cryogenic immersion microscope (WO/2006/113916) and the cryo-tomography X-ray microscope stage (US-2009-0129543-A1).

**References**

- 1 Kirkpatrick, P. and Baez, A.V. (1948) Formation of optical images by X-rays. *J. Optical Soc. Am.* 38, 766–774
- 2 Schmah, G. *et al.* (1996) Diffraction optics for X-ray imaging. *Microelectr. Eng.* 32, 351–367
- 3 Schmah, G. *et al.* (1993) X-ray microscopy studies. *Optik* 93, 95–102

<sup>a</sup> SXT microscopes are either under construction or being considered at the following synchrotron light sources: Elettra (<http://www.elettra.trieste.it/>), Diamond (<http://www.diamond.ac.uk/>), ALBA (<http://www.cells.es/>), and SOLEIL (<http://www.synchrotron-soleil.fr/>).



- 4 Kirz, J. *et al.* (1995) Soft X-ray microscopes and their biological applications. *Quart. Rev. biophys.* 28, 33–130
- 5 Attwood, D.T. (1999) *Soft X-rays and Extreme Ultraviolet Radiation: Principles and Applications*, Cambridge University Press
- 6 Meyer-Ilse, W. *et al.* (2001) High resolution protein localization using soft X-ray microscopy. *J. Microsc.* 201, 395–403
- 7 Schneider, G. (1997) Zone plates with high efficiency in high orders of diffraction described by dynamical theory. *Appl. Phys. Lett.* 71, 2242–2244
- 8 Schneider, G. (1998) Cryo X-ray microscopy with high spatial resolution in amplitude and phase contrast. *Ultramicroscopy* 75, 85–104
- 9 Le Gros, M.A. *et al.* (2005) X-ray tomography of whole cells. *Current Opinion in Structural Biology* 15, 593–600
- 10 Larabell, C. and Le Gros, M. (2004) Whole cell cryo X-ray tomography and protein localization at 50 micron resolution. *Biophys. J.* 86, 185A
- 11 Weiss, D. (2000). Computed Tomography Based on Cryo X-ray Microscopic Images of Unsectioned Biological Specimens. Georg-August University of Göttingen
- 12 Weiss, D. *et al.* (2000) Computed tomography of cryogenic biological specimens based on X-ray microscopic images. *Ultramicroscopy* 84, 185–197
- 13 Leis, A. *et al.* (2009) Visualizing cells at the nanoscale. *Trends Biochem. Sci.* 34, 60–70
- 14 Andersen, E.H. *et al.*, eds (1999) *Nanofabrication of X-ray ZonePlates with the Nanowriter Electron-Beam Lithography System.*, American Institute of Physics
- 15 Schmahl, G. *et al.* (1984) High-resolution X-ray microscopy with zone plate microscopes. *J. Phys. Paris* 45, 77–81
- 16 Hildebrand, M. *et al.* (2009) 3D imaging of diatoms with ion-abrasion scanning electron microscopy. *J. Struct. Biol.* 166, 316–328
- 17 Denbeaux, G. *et al.* (2001) Soft X-ray microscopy to 25 nm with applications to biology and magnetic materials. *Nucl. Instrum. Methods A* 467, 841–844
- 18 Natterer, F. (1986) *The Mathematics of Computerized Tomography*, Wiley
- 19 Baumeister, W. *et al.* (1999) Electron tomography of molecules and cells. *Trends Cell Biol.* 9, 81–85
- 20 Crowther, R.A. *et al.* (1970) 3 Dimensional reconstructions of spherical viruses by Fourier synthesis from electron micrographs. *Nature* 226, 421–425
- 21 Crowther, R.A. *et al.* (1970) Reconstruction of 3 dimensional structure from projections and its application to electron microscopy. *Proc. Roy. Soc. A* 317, 319–340
- 22 Schmahl, G. *et al.* (1995) Phase contrast studies of biological specimens with the x-ray microscope at BESSY (invited). *Rev. Sci. Instrum.* 66, 1282–1286
- 23 Schneider, G. *et al.* (1995) Cryo X-ray microscopy. *Synchrotron Rad. News* 8, 19–28
- 24 Larabell, C.A. and Le Gros, M.A. (2004) X-ray tomography generates 3-D reconstructions of the yeast, *Saccharomyces cerevisiae*, at 60-nm resolution. *Mol. Biol. Cell* 15, 957–962
- 25 Weiss, D. *et al.* (2001) Tomographic imaging of biological specimens with the cryo transmission X-ray microscope. *Nuclear Instrum. Methods Phys.Res. A* 467, 1308–1311
- 26 Schneider, G. *et al.* (2005) Novel X-ray microscopes for 3-D and fs-imaging at BESSY. *Proc. 8th Int. Conf. X-ray Microsc.* 7, 349–352
- 27 Parkinson, D.Y. *et al.* (2008) Quantitative 3-D imaging of eukaryotic cells using soft X-ray tomography. *J. Struct. Biol.* 162, 380–386
- 28 Gu, W.W. *et al.* (2007) X-ray tomography of *Schizosaccharomyces pombe*. *Differentiation* 75, 529–535
- 29 Le Gros, M.A. *et al.* (2009) High-aperture cryogenic light microscopy. *J. Microsc.-Oxford* 235, 1–8
- 30 Takman, P.A.C. *et al.* (2007) High-resolution compact X-ray microscopy. *J. Microsc.-Oxford* 226, 175–181
- 31 Bertillon, M. *et al.* (2009) High-resolution computed tomography with a compact soft x-ray microscope. *Optics Express* 17, 11057–11065
- 32 Chao, W.L. *et al.* (2005) Soft X-ray microscopy at a spatial resolution better than 15 nm. *Nature* 435, 1210–1213
- 33 Guttman, P. *et al.* (2001) Instrumentation advances with the new X-ray microscopes at BESSY II. *Nucl. Instrum. Meth. A* 467, 849–852
- 34 Niemann, B. *et al.* (2001) A rotating condenser and off-axis zone plate monochromator for the TXM at the undulator U41 at BESSY II. *Nucl. Instrum. Meth. A* 467, 857–860
- 35 Attwood, D. *et al.* (2006) Imaging at high spatial resolution: soft X-ray microscopy to 15 nm. *J. Biomed. Nanotechnol.* 2, 75–78
- 36 Kremer, J.R. *et al.* (1996) Computer visualization of three-dimensional image data using IMOD. *J. Struct. Biol.* 116, 71–76
- 37 Hohn, M. *et al.* (2007) SPARX, a new environment for Cryo-EM image processing. *J. Struct. Biol.* 157, 47–55
- 38 Spector, D.L. *et al.* (1998) *In Cells: A Laboratory Manual* (Vol.3), CSHL Press
- 39 Ashcroft, J.M. *et al.* (2008) TiO<sub>2</sub> nanoparticles as a soft X-ray molecular probe. *Chem. Commun.* 21, 2471–2473
- 40 Tsien, R.Y. (2005) Building and breeding molecules to spy on cells and tumors. *FEBS Lett.* 579, 927–932
- 41 Giepmans, B.N. *et al.* (2006) The fluorescent toolbox for assessing protein location and function. *Science* 312, 217–224